

RESEARCH ARTICLE

Channel characteristics of ultra-wideband systems with single co-channel interference

Chien-Ching Chiu*, Chun-Liang Liu and Shu-Han Liao

Department of Electrical Engineering, Tamkang University, Tamsui 25137, Taiwan

ABSTRACT

In this paper, the channel characteristics of ultra-wideband systems with single co-channel interference are investigated. A ray-tracing technique is developed to calculate channel frequency responses in an indoor environment, of which the frequency dependence for the dielectric constant and the conductivity are carefully considered. By using the frequency responses, the channel capacities with single co-channel interference are calculated. The outage probability of the channel capacities are also calculated for analyzing the channel statistical property. Furthermore, some useful channel statistical parameters are also investigated for different material partitions. Copyright © 2011 John Wiley & Sons, Ltd.

KEYWORDS

ultra-wideband; channel characteristic; ray-tracing technique

*Correspondence

Chien-Ching Chiu, Department of Electrical Engineering, Tamkang University, 151 Ying-chuan Road, Tamsui 25137, Taiwan.

E-mail: chiu@ee.tku.edu.tw

1. INTRODUCTION

Ultra-wideband (UWB) system, which can offer high bit rates availability, low power consumption, low costs, and high accuracy positioning capabilities, is one of the possible solutions for future short-range indoor data communication applications [1,2]. For indoor communications, a power spectral density of -41.3 dBm/MHz is allowed in the frequency band between 3.1 and 10.6 GHz by the Federal Communications Commission regulation for UWB systems [3]. One of the key differences between UWB systems and conventional narrowband systems lies in the frequency dependence of the transfer function because of a very wide band for UWB systems. In other words, the channel characteristics of conventional narrowband systems are different from that of UWB systems. Some studies about channel characteristics of UWB systems have been published [4–6]. An overview of reported measurements and modeling of the UWB systems in indoor environments are presented in [4] and [5]. In [6], the work of channel modeling for UWB systems is summarized.

For wireless communication systems, two main sources of performance degradation are the thermal noise present in the channel or generated in the receiver and unwanted signals emanating from the same or nearby stations. Co-channel interferences are one of the unwanted signals

and it appears when there are some transmitters with the same system nearby the receiver. Several studies have been made on effects of co-channel interference in wireless communication systems. One common point from these literatures is that the co-channel interferences are regarded as some kinds of statistical random variables (e.g., Gaussian or Nakagami) [7–11]. This statistical assumption is correct when a lot of co-channel interferences are received at the same time. However, this statistical assumption is not suitable for just few co-channel interferences. In indoor wireless communication systems, co-channel interferences are probably just caused by an adjacent room. As a result, the co-channel interferences expressed as statistical random variables are not correct in this situation. To the best of our knowledge, there is no paper that deals with the channel characteristics of UWB systems with single co-channel interference.

In this paper, a comparison of UWB communication characteristics with single co-channel interference for various materials of partitions in real environments is investigated. The effects of different materials of partitions with brick board, cloth office partition, concrete block, dry-wall, plywood, structure wood, and styrofoam on the UWB communication characteristics with single co-channel interference are presented. The ray-tracing method implemented in these simulations is developed by our laboratory. Different values of dielectric constant and conductivity of

materials for different frequency are carefully considered in channel calculation. The values of the dielectric constant and the conductivity of these materials versus operating frequency was discussed in [12]. Results of this research provide valuable insights into the channel capacity and root mean square (RMS) delay spread and so forth in the UWB communication system with signal co-channel interference. The remainder of this paper is organized as follows. In Section 2, channel modeling and formula description are presented. Several numerical results are included in Section 3, whereas Section 4 concludes the paper.

2. CHANNEL MODELING AND FORMULA DESCRIPTION

2.1. Channel modeling

The shooting and bouncing ray/image method can deal with high frequency radio wave propagation in the complex indoor environments [13,14]. It conceptually assumes that many triangular ray tubes are shot from the transmitting antenna (TX), and each ray tube bouncing and penetrating in the environments is traced in the indoor multi-path channel. If the receiving antenna (RX) is within a ray tube, the ray tube will have contributions to the received field at the RX, and the corresponding equivalent source (image) can be determined. By summing all contributions of these images, we can obtain the total received field at the RX. In the real environment, external noise in the channel propagation has been considered. The depolarization yielded by multiple reflections, refraction, and first order diffraction is also taken into account in our simulations. Note that the different values of dielectric constant and conductivity of materials for different frequency are carefully considered in channel modeling.

Using ray-tracing techniques to predict channel characteristics is effective and fast [13–15]. Thus, a ray-tracing channel model is developed to calculate the channel matrix of UWB systems. Flow chart of the ray-tracing process is shown in Figure 1. It conceptually assumes that many triangular ray tubes (not rays) are shot from a transmitter. Here, the triangular ray tubes whose vertexes are on a sphere are determined by the following method. First, we construct an icosahedron, which is made of 20 identical equilateral triangles [16]. Then, each triangle of the icosahedron is tessellated into a lot of smaller equilateral triangles. Finally, these small triangles are projected on to the sphere, and each ray tube whose vertexes are determined by small equilateral triangles is constructed.

For each ray tube bouncing and penetrating in the environments, we check whether reflection times and penetration times of the ray tube are larger than the numbers of maximum reflection N_{ref} and maximum penetration N_{pen} , respectively. If it is not, we check whether the receiver falls within the reflected ray tube. If it does, the contribution of

the ray tube to the receiver can be attributed to an equivalent source (i.e., image source). In other words, a specular ray going to the receiver exists in this tube, and this ray can be thought as launched from an image source. Moreover, the field diffracted from illuminated wedges of the objects in the environment is calculated by uniform theory of diffraction [17]. Note that only the first diffraction is considered in this paper because the contribution of the second diffraction is very small in the analysis.

By using these images and received fields, the channel frequency response can be obtained as

$$H(f) = \sum_{p=1}^{N_p} a_p(f) e^{j\theta_p(f)} \quad (1)$$

where p is the path index, N_p is the number of paths, f is the frequency of sinusoidal wave, $\theta_p(f)$ is the p th phase shift, and $a_p(f)$ is the p th receiving magnitude. Note that the channel frequency response of UWB systems can be calculated by Equation (1) in the frequency range of UWB systems for both desired signal and interference signal.

2.2. Channel capacity

On the basis of the Shannon–Hartley theorem, channel capacity is a function of average received signal power P_r , average noise power P_n , and bandwidth W for a flat narrowband additive white Gaussian noise system [18], and the channel capacity can be stated as

$$C = W \log_2 \left(1 + \frac{P_r}{P_n} \right) \quad (2)$$

The channel capacity with single co-channel interference in a multipath channel is calculated as

$$C = W \log_2 \left(1 + \frac{P_u \times G_u}{(P_i \times G_i) + P_n} \right) \quad (3)$$

where P_u and P_i are the transmitting powers of the useful source and the interference source, respectively. $G_u = |H_u(f)|^2$ and $G_i = |H_i(f)|^2$ are the power gains of the channel for the useful source and the interference source, respectively.

For further analysis of channel capacity in multipath channels with single co-channel interference, Equation (3) is rearranged as follows. The right term both in numerator and denominator inside the parentheses is divided by P_n first; thus, Equation (3) can be expressed as

$$C = W \log_2 \left(1 + \frac{\frac{P_u}{P_n} \times G_u}{\left(\frac{P_i}{P_n} \times G_i \right) + 1} \right) \quad (4)$$

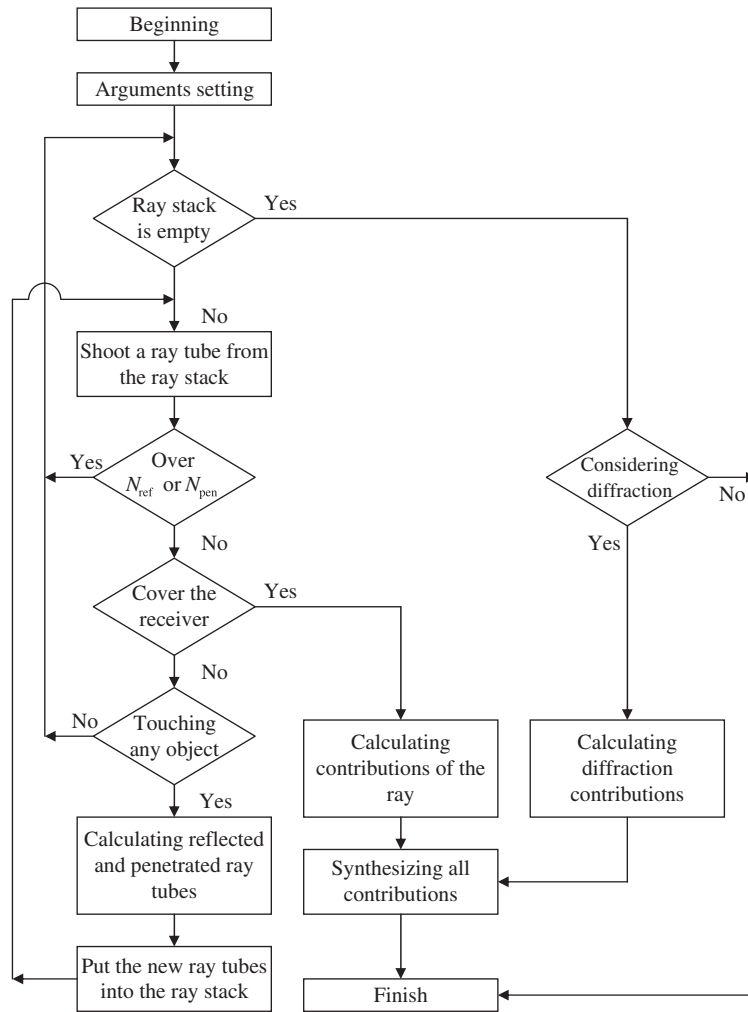


Figure 1. Flow chart of the ray-tracing process.

The equation is further modified that it takes P_i/P_n times P_u/P_u ; thus, it can be rewritten as

$$C = W \log_2 \left(1 + \frac{\frac{P_u}{P_n} \times G_u}{\left(\frac{P_i}{P_n} \times \frac{P_u}{P_u} \times G_i \right) + 1} \right) \quad (5)$$

The equation is finally rearranged as

$$C = W \log_2 \left(1 + \frac{SNR \times G_u}{1 + (SIR^{-1} \times SNR \times G_i)} \right) \text{ (bits/s)} \quad (6)$$

where SNR is transmitting power to noise power ratio and SIR^{-1} is the inverse of transmitting power to transmitting interference power. Note that, as indicated in Equation (6), the channel capacity is a function of SNR , SIR^{-1} , G_u , and G_i .

It is possible to divide a wideband channel into several narrowband channels [19]. As a result, the channel capacity of UWB systems is calculated as the summation of

the channel capacities of flat narrowband systems at each discrete frequency component. Thus, the channel capacity (bandwidth efficiency) can be written as

$$C^{UWB} = \frac{1}{BW} \sum_{k=1}^{N_f} C_k \text{ (bits/s/Hz)} \quad (7)$$

where BW is the bandwidth of UWB, N_f is the number of frequency components and C_k is the channel capacity in the k th discrete frequency component.

Furthermore, in the practical communication systems, it is important to investigate the channel capacity in the sense of outage probability. An outage probability is defined as the event that the communication channel does not support a target data rate. If we give a data rate R , then the outage probability can be written as

$$P_o = P \left\{ C^{UWB} < R \right\} \quad (8)$$

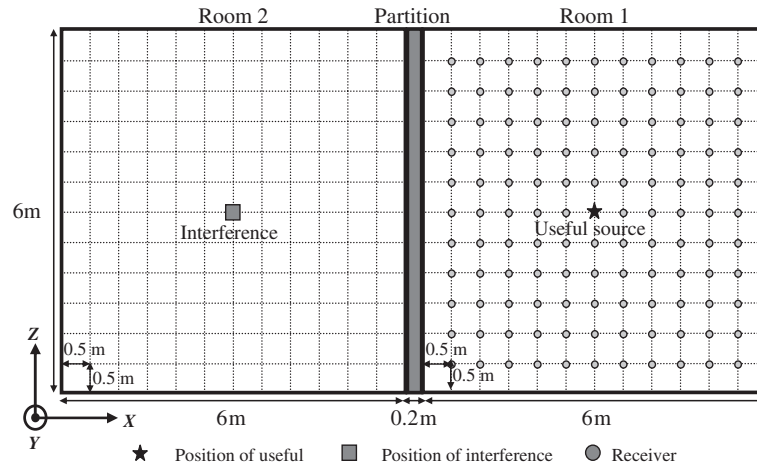


Figure 2. The top view of the simulation environment.

Table I. Dielectric constants and conductivities versus frequencies for brick block and drywall.

Frequency (GHz)	Brick block		Drywall	
	Dielectric constants ϵ_r	Conductivities σ (S/m)	Dielectric constants ϵ_r	Conductivities σ (S/m)
3.0	3.9000	4.55E-02	2.4200	2.02E-04
3.5	4.0000	5.37E-02	2.4200	3.76E-04
4.0	4.1000	6.20E-02	2.4200	5.38E-04
4.5	4.1750	6.99E-02	2.4200	9.08E-04
5.0	4.2500	7.79E-02	2.4200	1.34E-03
5.5	4.3250	8.59E-02	2.4100	1.84E-03
6.0	4.4000	9.39E-02	2.4100	2.41E-03
6.5	4.4250	1.02E-01	2.4000	3.03E-03
7.0	4.4750	1.11E-01	2.4000	3.73E-03
7.5	4.5500	1.21E-01	2.3900	4.48E-03
8.0	4.6250	1.32E-01	2.3900	5.31E-03
8.5	4.7000	1.42E-01	2.3800	6.18E-03
9.0	4.7750	1.53E-01	2.3800	5.95E-03
9.5	4.8500	1.64E-01	2.3700	8.13E-03
10.0	4.9250	1.75E-01	2.3700	7.90E-03

2.3. Statistical channel parameters

By Hermitian processing and inverse fast Fourier transform [20], the channel impulse response are calculated using four statistical channel parameters for UWB systems [6] with single co-channel interference. The four parameters are the mean excess delay, the RMS delay spread, the number of significant paths within 10 dB from the peak ($NP_{10\text{dB}}$), and the number of significant paths capturing 85% of energy in channel ($NP_{85\%}$), respectively.

The mean excess delay and RMS delay spread are the most commonly used to analyze dispersive properties of time in multipath channel. The mean excess delay is the first moment of the power delay profile and is defined as

$$\bar{\tau} = \frac{\sum_K p(\tau_k) \tau_k}{\sum_K p(\tau_k)} \quad (9)$$

where τ_k is the k th delay time relative to the first detectable signal arriving at the receiver at $\tau_0 = 0$ and $p(\tau_k)$ is the power at τ_k . The RMS delay spread is the square root of the second central moment of the power delay profile and is defined as

$$\sigma_\tau = \sqrt{\bar{\tau}^2 - (\bar{\tau})^2} \quad (10)$$

where

$$\bar{\tau}^2 = \frac{\sum_K p(\tau_k) \tau_k^2}{\sum_K p(\tau_k)} \quad (11)$$

The $NP_{10\text{dB}}$ and the $NP_{85\%}$ are useful parameters that can be utilized to calculate how many significant paths are need. The criterion of the $NP_{10\text{dB}}$ is to compute how many numbers of significant paths within 10 dB of the peak of

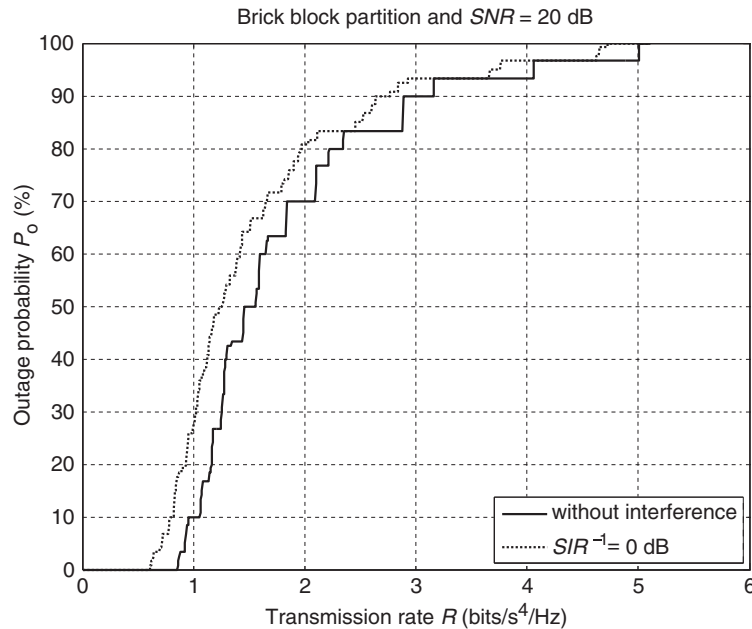


Figure 3. Outage probabilities versus transmission rates for brick block partition with and without interference. The solid curve and the dash curve denote the cases with and without interference, respectively. SIR, signal-to-interference ratio; SNR, signal-to-noise ratio.

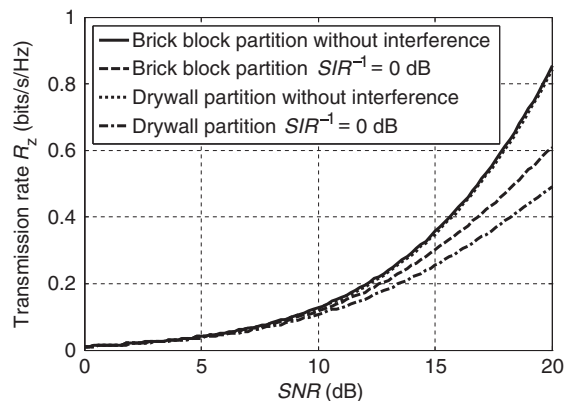


Figure 4. The values of R_z versus SNR for brick block partition/drywall partition with and without interference. The solid curve and the dash curve denote the cases with and without interference, respectively. SIR, signal-to-interference ratio; SNR, signal-to-noise ratio.

amplitude. The criterion of the $NP_{85\%}$ is to compute how many numbers of significant paths capture more than 85% of the channel's total energy.

3. NUMERICAL RESULTS

Simulation scenarios and numerical results are presented in this section. A ray-tracing technique is developed to calculate the channel frequency response from 3.1 to 10.6 GHz with a frequency interval of 5 MHz. That is, 1501 frequency components are used. The top view of the

simulation environment is shown in Figure 2. There are two adjacent rooms, Room 1 and Room 2, with a partition between them. The dimensions of the two rooms are both 6.0 m (length) \times 3.0 m (height) \times 6.0 m (width), and the partition has a dimension of 6.0 m (length) \times 3.0 m (height) \times 0.2 m (thickness).

The materials used for the ceiling, the walls, and the ground are concrete blocks. However, the material of the partition is changeable in our simulation. The dielectric constant and conductivity of all objects in the simulation environment are dependent on the operating frequency for UWB systems, which the values of the dielectric constant and conductivity of these materials versus operating frequency can be found in reference [12]. For example, the relative dielectric constants and conductivities versus frequencies for brick block and drywall are shown in Table I.

The transmitter of the useful source (9.2 m, 1.0 m, 3.0 m) is located at the center of Room 1, and the transmitter of interference source (3.0 m, 1.0 m, 3.0 m) is located at the center of Room 2. There are 120 receivers located in Room 1 with an equal distance of 0.5 m. Note that there is just a little effect on statistical channel properties if we set more receivers in Room 1. Furthermore, all the antenna heights of these receivers are chosen as 1 m for a laptop located on the desk, and the polarizations of both TX and RX are vertical.

3.1. Numerical results for channel capacity

The outage probabilities of channel capacity versus transmission rate with and without single co-channel interference for brick block partition are shown in Figure 3. Here,

Table II. Values of K_1 and R_z for seven material partitions at $SNR = 20$ dB with and without interference.

Partition type	Parameters and condition			
	K_1 (dB)	R_z (bits/s/Hz)		
		Without interference	With interference	Difference
Brick block	7.8	0.8536	0.6082	0.2454
Cloth office partition	7.0	0.8076	0.5316	0.2760
Concrete block	8.0	0.8229	0.5827	0.2402
Drywall	6.2	0.8433	0.4907	0.3526
Plywood	7.4	0.8280	0.5827	0.2453
Structure wood	8.4	0.8178	0.5827	0.2351
Styrofoam	6.6	0.8024	0.4651	0.3373

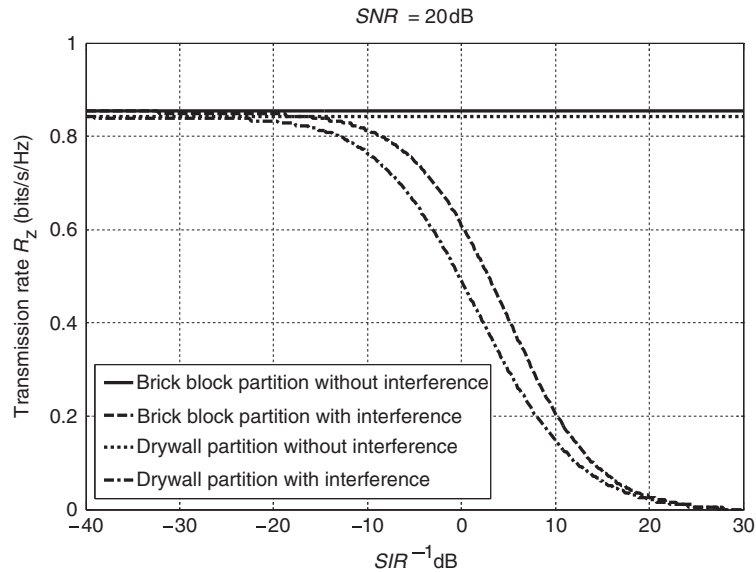


Figure 5. The values of R_z versus SIR^{-1} for brick block partition/drywall partition with and without interference. The solid curve and the dash curve denote the cases with and without interference, respectively. SIR, signal-to-interference ratio; SNR, signal-to-noise ratio.

$SNR = 20$ dB and $SIR^{-1} = 0$ dB are chosen. Note that $SIR^{-1} = 0$ dB means that the transmitting power of the interference source is the same as that of the useful source. R_z is defined as the transmission rate for zero outage probability. It is seen that the values of R_z are 0.8536 and 0.6082 bits/s/Hz for the case with and without interference, respectively. It is clear that the transmission rate degrades about 0.25 bits/s/Hz for brick block partition when single co-channel interference exists.

The values of R_z versus SNR are shown in Figure 4 for brick block partition and drywall partition. Note that, in the figure, there is no difference for the transmission rates with and without interference when SNR is below a value of K_1 . Here, K_1 is defined as the maximum SNR when the transmission rate with interference is the same as that without interference. The values of K_1 are 7.8 and 6.2 dB for brick block partition and drywall partition, respectively. Note that the noise power is far larger than

Table III. Values of K_2 for seven material partitions.

Partition type	K_2 (dB)
Brick block	-9.8
Cloth office partition	-11.8
Concrete block	-9.6
Drywall	-13.6
Plywood	-10.2
Structure wood	-9.4
Styrofoam	-13.0

the interference power when SNR is lesser than K_1 and the interference could be ignored. Furthermore, a smaller value of K_1 implies that the interference is larger. The values of R_z for brick block partition at $SNR = 20$ dB with and without interference are 0.6082 and 0.8536 bits/s/Hz, respectively. The values for drywall partition are 0.4907

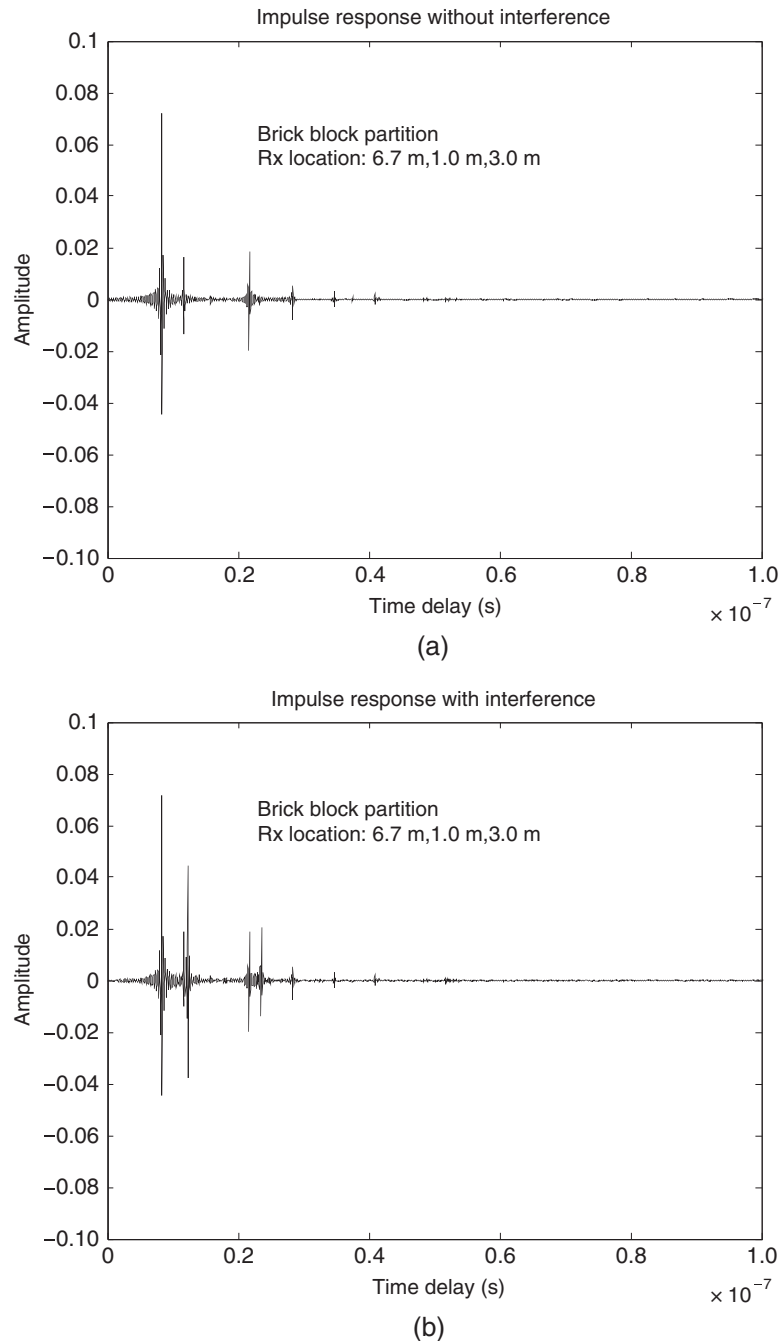


Figure 6. (a) The channel impulse response without interference. (b) The channel impulse response with interference.

and 0.8433 bits/s/Hz. The values of K_1 and R_z for seven material partitions at $SNR = 20$ dB with and without interference are listed in Table II. It is shown that the interference is the largest for drywall partition and is the smallest for structural wood.

The values of R_z versus SIR^{-1} at a fixed $SNR = 20$ dB for brick block partition and drywall partition are shown in Figure 5. Note that, in the figure, there is almost no

difference for the transmission rate with and without interference when SIR^{-1} is below a value of K_2 . Here, K_2 is defined as the value of the SIR^{-1} when the transmission rate with interference is the same as the 95% of the transmission rate without interference. The values of K_2 are -9.8 and -13.6 dB for brick block partition and drywall partition, respectively. Note that the interference power could be ignored when SIR^{-1} is lesser than the

Table IV(a). Values of the mean excess delay and root mean square delay spread for seven material partitions with and without interference.

Partition type	Parameters and condition			
	Mean excess delay (ns)		Root mean square delay spread (ns)	
	Without interference	With interference	Without interference	With interference
Brick block	1.27	2.54	8.90	9.50
Cloth office partition	1.08	2.50	8.75	9.52
Concrete block	1.14	2.33	8.79	9.32
Drywall	1.22	3.81	8.97	11.19
Plywood	1.17	2.35	8.81	9.25
Structure wood	1.14	2.43	8.79	9.49
Styrofoam	1.14	3.73	8.99	11.00

Table IV(b). Values of NP_{10dB} and $NP_{85\%}$ for seven material partitions with and without interference.

Partition type	Parameters and condition			
	NP_{10dB}		$NP_{85\%}$	
	Without interference	With interference	Without interference	With interference
Brick block	3.28	4.25	8.59	12.8
Cloth office partition	3.22	4.08	7.57	13.38
Concrete block	3.25	4.06	7.90	11.63
Drywall	3.23	4.56	8.11	23.75
Plywood	3.25	4.07	8.07	11.78
Structure wood	3.23	4.17	7.87	12.27
Styrofoam	3.21	4.89	7.62	20.41

value of K_2 . Contrary to the value of K_1 , a larger value of K_2 shows that the interference is larger. The values of K_2 for seven material partitions are listed in Table III. It is concluded that the degradation of channel capacity with interference is the largest for drywall partition and is the lowest for structural wood partition.

3.2. Numerical results for four statistical channel parameters

By channel impulse responses, four statistical channel parameters are calculated with and without single co-channel interference for seven material partitions. The transmitting power for the interference source is set as that for the useful source in the following calculation. The channel impulse responses for a location of Rx (3.7 m, 1.0 m, 3.0 m) without and with interference are plotted in Figure 6(a) and Figure 6(b), respectively. It is found that the multipath effect for the channel impulse response with interference is more severe due to the co-channel interference.

The average values of mean excess delay and RMS delay spread with and without interference are listed in Table IV(a), and the average values of NP_{10dB} and $NP_{85\%}$ with and without interference are listed in Table IV(b). It is found that the values of the four parameters with interference for drywall partition and styrofoam partition are larger than that for the others. It is concluded

that the materials of good penetration ability such as drywall and styrofoam have stronger magnitude of interference and cause longer time dispersion. Moreover, they also increase the number of significant paths.

4. CONCLUSIONS

A research on the channel characteristics of UWB systems with single co-channel interference has been presented. Not only channel capacity but also four channel parameters are calculated to analyze an environment of two rooms with a partition. Numerical results show that the degradation of channel capacity with interference is the largest for drywall partition and is the lowest for structural wood partition. Numerical results also indicate that the materials of good penetration ability such as drywall and styrofoam have stronger magnitude of interference and cause longer time dispersion. Moreover, they also increase the number of significant paths. Finally, it is worth noting that in our researches, the present work provided not only comparative information but also quantitative information.

REFERENCES

1. Yang L, Giannakis GB. Ultra-wideband communications: an idea whose time has come. *IEEE Signal Processing Magazine* 2004; **21**(6): 26–54.

2. Roy S, Foerster JR, Somayazulu VS, Leeper DG. Ultrawideband radio design: the promise of high-speed, short-range wireless connectivity. *Proceedings of the IEEE* 2004; **92**(2): 295–311.
3. Federal Communications Commission. FCC notice of proposed rule making, revision of part 15 of the commission's rules regarding ultra-wideband transmission systems, 2000. Federal Communications Commission (FCC), Washington, DC, ET-Docket 98–153.
4. Irahauten Z, Nikoosar H, Janssen GJM. An overview of ultra wide band indoor channel measurements and modeling. *IEEE Microwave and Wireless Components Letters* 2004; **14**(8): 386–388.
5. Molisch AF. Ultrawideband propagation channels—theory, measurement, and modeling. *IEEE Transactions on Vehicular Technology* 2005; **54**(5): 1528–1545.
6. Foerster JR. Channel modeling sub-committee report final, 2002. Technical Report. P802.15-02/368r5-SG3a, IEEE P802.15 SG3a Contribution.
7. Song Y, Blostein SD, Cheng J. Outage probability comparisons for diversity systems with cochannel interference in Rayleigh fading. *IEEE Transactions on Wireless Communications* 2005; **4**(4): 1279–1284.
8. Yang L, Alouini M-S. Performance comparison of different selection combining algorithms in presence of co-channel interference. *IEEE Transactions on Vehicular Technology* 2006; **55**(2): 559–571.
9. Shah A, Haimovich AM, Simon MK, Alouini M-S. Exact bit-error probability for optimum combining with a Rayleigh fading Gaussian cochannel interferer. *IEEE Transactions on Communications* 2000; **48**(6): 908–912.
10. Shah A, Haimovich Am. Performance analysis of maximal ratio combining and comparison with optimum combining for mobile radio communications with cochannel interference. *IEEE Transactions on Vehicular Technology* 2000; **49**(4): 1454–1463.
11. Sagias NK, Karagiannidis GK, Zogas DA, Tombras GS, Kotsopoulos SA. Average output SINR of equal-gain diversity in correlated Nakagami- m fading with cochannel interference. *IEEE Transactions on Wireless Communications* 2005; **4**(4): 1407–1411.
12. Muqaibel A, Safaai-Jazi A, Bayram A, Attiya AM, Riad SM. Ultrawideband through-the-wall propagation. *IEE Proceedings—Microwaves, Antennas and Propagation* 2005; **152**(6): 581–588.
13. Chen SH, Jeng SK. An SBR/image approach for indoor radio propagation in a corridor. *IEICE Transactions on Electronics* 1995; **E78-C**: 1058–1062.
14. Chen SH, Jeng SK. SBR image approach for radio wave propagation in tunnels with and without traffic. *IEEE Transactions on Vehicular Technology* 1996; **45**: 570–578.
15. Loredó S, Rodríguez-Alonso A, Torres RP. Indoor MIMO channel modeling by rigorous GO/UTD-based ray tracing. *IEEE Transactions on Vehicular Technology* 2008; **57**(2): 680–692.
16. Wenninger MJ. *Spherical Models*. New York: Cambridge University Press, 1979.
17. Balanis CA. *Advanced Engineering Electromagnetics*. John Wiley & Sons: Hoboken, NJ, 1989.
18. Shannon CE. A Mathematical Theory of Communication. *Bell System Technical Journal* 1948; **27**: 379–423, 623–657.
19. Cover TM, Thomas JA. *Elements of Information Theory (Wiley Series in Telecommunications and Signal Processing)*. John Wiley & Sons: Hoboken, NJ, 1991.
20. Oppermann I, Hämäläinen M, Iinatti J. *UWB Theory and Applications*. John Wiley & Sons: Hoboken, NJ, 2004.

AUTHORS' BIOGRAPHIES



Chien-Ching Chiu received his BSCE degree from National Chiao Tung University, Hsinchu, Taiwan, in 1985 and his MSEE and PhD degrees from National Taiwan University, Taipei, in 1987 and 1991, respectively. From 1987 to 1989, he was a communication officer with the ROC Army Force. In 1992 he joined the faculty of the Department of Electrical Engineering, Tamkang University, where he is now a professor. From 1998 to 1999, he was a visiting scholar at the Massachusetts Institute of Technology, Cambridge, and the University of Illinois at Urbana-Champaign. He was a visiting professor with the University of Wollongong, Australia, in 2006. His current research interests include microwave imaging, numerical techniques in electromagnetics, indoor wireless communications, and ultrawideband communication systems.



Chun-Liang Liu was born in Taipei, Taiwan, Republic of China, on April 20, 1980. He is working toward his Ph.D. degree in the Department of Electrical Engineering, Tamkang University. His current research interests include wireless communication systems, ultra-wideband systems, and MIMO systems.



Shu-Han Liao was born in Taipei, Taiwan, Republic of China, on September 18, 1982. He received the M.S.C.E. degree from Feng Chia University in 2008, and now is working toward Ph.D degrees in the Department of Electrical Engineering, Tamkang University. His current research interests include indoor

wireless communication systems, ultra-wideband systems, and MIMO systems.